

## Validation of FLUENT against incompressible and compressible flow through orifices

Q G RAYER BSc, DPhil, CPhys and G D SNOWSILL BSc, MIMechE  
Fluid Systems Group, Rolls-Royce plc, Derby, UK

Validation against air systems problems is required to enable CFD codes to be confidently used in the design of turbine cooling air systems. CFD calculations of orifice and slit discharge coefficients ( $C_d$ ) have been compared with measured and theoretical values. The literature details quantitative data for these cooling system elements. The turbulence model used critically affected the accuracy of incompressible calculations for a 0.5 aspect ratio orifice. Although commonly used in engines, this aspect ratio caused difficulties in accurately simulating flow reattachment. Sharp-edged slit compressible  $C_d$  calculations agreed with theory to 4%. These results give confidence that CFD will become a valuable tool for evaluating air system losses in novel configurations.

### NOTATION

A	Area of duct inlet, $m^2$ in three-dimensions, $m^2$ per meter in two-dimensions.
$A_r$	Orifice area, $m^2$ in three-dimensions.
$C_d$	Discharge coefficient $\equiv W_{\text{actual}}/W_{\text{ideal}}$ .
d	Orifice diameter of slit width, m.
p	Static pressure, Pa.
$p_i$	System inlet static pressure, Pa.
$p_o$	System outlet static pressure, Pa.
$p_{\text{ref}}$	Reference pressure, $10^5$ Pa.
P	Total pressure, subscripted notation as for 'p', Pa.
Q	Mass flow function, $W.T^{1/2}.(AP)^{-1}$ .
Re	Reynolds number $\equiv W_T d.(A_r \mu)^{-1}$ .
t	Orifice thickness, m.
T	Air temperature, K.

$u_\tau$	$=(\tau_w/\rho)^{1/2}$ , the friction velocity.
$U_{\max}$	Maximum air velocity achieved in simulation, $\text{m}\cdot\text{s}^{-1}$
$W$	Mass flow rate, $\text{kg}\cdot\text{m}^{-3}$ .
$W_{\text{actual}}$	Mass flow rate achieved through system as calculated by FLUENT, $\text{kg}\cdot\text{s}^{-1}$ .
$W_{\text{ideal}}$	Theoretically predicted mass flow, $\text{kg}\cdot\text{s}^{-1}$ .
$W_T$	Total air mass flow rate through duct, $\text{kg}\cdot\text{m}^{-3}$ .
$y_p$	Distance from wall to cell centre.
$y^+$	$\equiv \rho u_\tau y_p \cdot \mu^{-1}$ , wall units.
$\Delta p$	System pressure drop, Pa.
$\mu$	Air viscosity at duct inlet, $2 \times 10^{-5} \text{kg}\cdot\text{m}^{-1}\cdot\text{s}^{-1}$ .
$\rho$	Air density, $1.225 \text{kg}\cdot\text{m}^{-3}$ for incompressible flow.
$\tau_w$	Wall shear stress.

## 1 INTRODUCTION

Gas turbine internal cooling air systems perform several functions, of which the most important are turbine blade/vane cooling, ventilation of rotating components and the sealing of turbine cavities against hot core flow gas ingress. These functions are critically important in ensuring the integrity of highly stressed rotating components. A significant proportion of the total core mass flow is used in the internal air system with a consequent increase in turbine entry temperature at take-off conditions, and of specific fuel consumption at cruise. In order to minimise running costs, it is essential that the flow delivered by the system matches the requirement as closely as possible.

Traditional methods of analysing gas turbine internal air systems have been to use one-dimensional network simulations. The representation of complex loss features has been by correlations representing empirical sources of data. These include standard sources such as ESDU(3), published literature and, for features particular to gas turbines, specially commissioned research data. This is unsatisfactory for two reasons:

1. Practical considerations mean that it is often inconvenient to design loss features in the same way as the ideal geometries tested by researchers.
2. The market is extremely competitive, making it undesirable to support extensive research activity unless there is no alternative.

It is clearly very important to develop new methods of deriving losses which allow better use to be made of research data and allow novel components to be investigated.

Computational Fluid Dynamics (CFD) simulations offer the prospect of rapid and accurate solution of turbine cooling air system problems. To give confidence that CFD calculations will prove sufficiently accurate for use within Rolls-Royce, and to establish guidelines for CFD code use, it is necessary to undertake a programme of code validation against relevant air systems problems. Quantitative solutions to a proven accuracy of better than 10% are required, with an accuracy of better than 5% being seen as highly desirable for static pressures, pressure differences, velocities and temperatures.

CFD calculations are carried out for complex geometries within Rolls-Royce to determine the relative merits of different gas turbine component configurations. In addition the critical significance of establishing the absolute quantitative accuracy of simulations has not been neglected. As a first step in a CFD validation programme against the absolute values of flow parameters for a range of geometries, the simplest possible relevant systems have been chosen for which quantitative data is available, commencing with air flow through an orifice. The results and methodology assist in the generation of a database of configurations solved to a known accuracy. As the programme continues the experience gained will contribute to accurate validation against flows in more complex geometries including ducts with side-wall apertures, rotor-stator systems and other configurations relevant to gas turbine applications, and for which Rolls-Royce has access to high-quality quantitative data. The experience gained, even for the simple orifice geometry, has shown that achieving absolute accuracies of (say) 5% is not as straightforward as might be expected. This is consistent with the experience of Hay and Lampard (1) for the more complex problem of modelling a hole in a rotating disc, where although relative  $C_d$  calculations gave good agreement, absolute values were about 15% lower than measurements.

Following this approach FLUENT/UNS version 1.4 (2) calculations have been validated against orifice  $C_d$ s. Additionally, data which allows a check to be carried out on the form of the flow field is extremely desirable. This has been done for the case of the compressible flow of air through a two-dimensional slit, where theoretical results gave an expression for the contraction ratio.

The results of the CFD calculations in two-dimensions have been compared with ESDU data (3) and theoretical predictions (4). Sensitivity studies have been carried out to explore the effects of different mesh configurations, mesh refinement and other factors.

## 1.1 FLUENT/UNS

FLUENT/UNS is a commercially available unstructured CFD code. It uses the finite volume method of discretisation over a non-staggered grid, with interpolation carried out by a first-order, second-order or power-law scheme. The discretised equations are solved by the SIMPLE algorithm using an iterative point-based Gauss-Seidel solver with multigrid acceleration.

## 1.2 Definitions

The orifice  $C_d$  is defined  $W_{\text{actual}}/W_{\text{ideal}}$ . For incompressible flow this becomes  $C_d = W_{\text{actual}} \cdot A_i^{-1} \cdot (2\rho \cdot \Delta p)^{-1/2}$ . For compressible flow,  $W_{\text{ideal}} = Q A_i p_i T^{-1/2}$ , where for unchoked flow

$$Q^2 = \frac{2}{R} \left( \frac{\gamma}{\gamma - 1} \right) \left[ \frac{\left( \frac{p_i}{p_{\text{ref}}} \right)^{\frac{\gamma-1}{\gamma}} - 1}{\left( \frac{p_i}{p_{\text{ref}}} \right)^{\frac{\gamma-1}{\gamma}}} \right] \left( \frac{p_i}{p_{\text{ref}}} \right)^{-\frac{2}{\gamma}}$$

### 1.3 Modelling Considerations

In some cases the converged CFD solution gave reversed flow at the system outlet. Such solutions were regarded as unacceptable and the results discarded.

The simulations used  $Re > 4000$  and so were considered to be turbulent. For both the  $k-\epsilon$  and Reynolds Stress turbulence models the thin turbulent boundary layers were simulated using wall functions. For the wall function correlations to apply the value of the parameter  $y^+$  must be in the range 30-100. Alternatively (as in this case) the solution can be demonstrated to be independent of the value of  $y^+$  obtained.

FLUENT/UNS includes a 'mesh adaption' capability, which allows the computational grid to be refined in regions selected by the user following a converged solution. Appropriate  $y^+$  values can be attained by solving the problem on an initial mesh and then calculating the  $y^+$  values for cells adjacent to the walls. Refinement can then be carried out on those individual cells which have a  $y^+$  greater than some specified value. This process of solution followed by adaption may be repeated until the user is satisfied with the quality of the solution obtained. A disadvantage of this approach is that it can be time-consuming to execute several successive runs of a problem, with local refinements following each converged solution.

All the simulations were executed in the steady-state.

## 2 INCOMPRESSIBLE FLOW THROUGH A 0.5 ASPECT RATIO ORIFICE

ESDU (3) allows  $C_d$  to be calculated for incompressible flow through a circular orifice. For a  $t/d=0.5$  aspect ratio orifice, with  $Re \geq 4000$ , the ESDU data gives  $C_d=0.703$ . The ESDU data was derived using a loss coefficient,  $k$  with a quoted accuracy of  $\pm 9.5\%$  over the range  $t/d=0$  to 0.8. For  $t/d=0.5$  the uncertainty in  $k$  is  $\pm 2.4\%$  leading to an uncertainty in  $C_d$  of  $\pm 1.2\%$ .

### 2.1 $k-\epsilon$ Turbulence Modelling

Simulations of the incompressible flow through an orifice were carried out using a two-dimensional axisymmetric mesh with the geometry shown in Figure 1. The boundary conditions were set as a total pressure inlet and static pressure outlet, with a reference pressure of  $10^5$  Pa. The inlet and outlet duct diameters were 6cm, with an inlet duct length of 10cm. The duct outlet length varied between 15 and 60cm, the upper limit giving 30 orifice diameters downstream of the orifice. The orifice thickness,  $t=1$ cm and diameter,  $d=2$ cm, giving  $t/d=0.5$ .

The model was meshed using between 352 and 18,400 quadrilateral cells and solved using both first and second order discretisation schemes. With a pressure difference of  $\Delta P=7.5$  kPa, mesh refinement was carried out by a combination of adaption based on  $y^+$  values and mesh doubling. The successive refinements over such a large range of cells demonstrated the grid independence of the solution and insensitivity to the ranges of  $y^+$  obtained. The effect on  $C_d$  of the successive refinements are shown in Figure 2. The parameter values for the densest

meshes are given in Table 1, with the mesh around the orifice lip shown in Figure 3. In all the cases run with the k- $\epsilon$  turbulence model the flow re-attached before leaving the orifice.

The FLUENT second-order discretisation scheme results with 18,400 cells gave  $C_d=0.7807$  (Table 1). 11% high compared with the ESDU data.

**Table 1: Axisymmetric Incompressible Orifice Flow using k- $\epsilon$  Turbulence Model (60cm Outlet Duct).**

Parameter	1st Order Scheme	2nd Order Scheme
Number of cells	18,400	18,400
$\Delta P$ , kPa	7.5	7.5
$p_{in}$ , Pa	7,489.7	7,490.5
$U_{max}$ , m.s <sup>-1</sup>	116.7	114.5
$W_{actual}$ , kg.s <sup>-1</sup>	0.03360	0.03335
$C_d$	0.7865	0.7807
Re	106,952	106,156
$y^+_{max}$	45	47

### *Sensitivity Studies*

A range of sensitivity studies was carried out to see if these would effect the value of  $C_d$  obtained using the k- $\epsilon$  turbulence model.

The duct outlet length was varied between 15 and 60cm. At the shorter outlet lengths the recirculation downstream of the orifice extended to the simulation outlet, resulting in unacceptable reversed flow on the 'pressure outlet' boundary. Beyond this the duct outlet length had little effect on the solution obtained.

The total pressure inlet boundary condition was changed to a fixed uniform velocity type. The inlet velocity was chosen to maintain the same mass flow as seen in the previous case. There was very little effect on the resulting solution. While it would have been desirable to execute an additional sensitivity study with a fully developed inlet velocity profile, this was not carried out. Instead it is hoped that the range of sensitivity studies carried out, including variations to the inlet turbulence intensity, would cover most of the conditions required.

The short inlet duct length of 10cm could mean that the turbulent flow was developing between the inlet and the orifice. To check for an effect from the inlet turbulence, the fixed turbulence intensity at the inlet was set to values of 0.2%, 10% and 20%. There was no significant effect on the solution obtained.

## **2.2 Reynolds Stress Turbulence Modelling**

Simulations were carried out using the Reynolds Stress Model (RSM) with  $\Delta P=7.5$ kPa. A number of different meshes were used with between 1,716 and 17,779 cells. In many cases a first or second-order discretisation scheme preliminary run with the k- $\epsilon$  turbulence model was executed as a starting-point for the RSM simulation. The RSM simulations gave much better

agreement with the ESDU  $C_d$ s. The resulting flow patterns showed that in the RSM streamlines did not re-attach before leaving the orifice, as they did in the k- $\epsilon$  model runs.

As a result of the range of studies carried out using the RSM a solution methodology using only 3,000-4,000 cells was evolved which gave  $C_d$ s which agreed with ESDU data to the required accuracy.

The resulting approach used a mesh of 3,738 cells with certain areas of the mesh refined in advance of solution by selecting regions around the orifice (Figure 4) to avoid the need for mesh adaption. The refinement placed particular emphasis on regions around the orifice lip (where separation occurs) and the orifice outlet (where re-attachment should not occur). An initial solution using the k- $\epsilon$  turbulence model with a second-order discretisation scheme, gave a good initialisation for a second-order RSM simulation.

The resulting RSM solution gave  $C_d=0.729$ , only 3.7% above ESDU. The streamlines, showing no re-attachment are plotted in Figure 5.

**Table 2: Results of Sensitivity Study Comparing Standard k- $\epsilon$  Turbulence Model with the RSM (2,472 cells).**

Parameter	k- $\epsilon$ Model		RSM
Discretisation scheme	1st Order	2nd Order	2nd Order
$C_d$	0.803	0.798	0.761
Difference from ESDU	14.2%	13.5%	8.3%
$U_{\max}$ , m.s <sup>-1</sup>	118.3	116.9	128.4
$W_{\text{actual}}$ , m.s <sup>-1</sup>	0.03430	0.03409	0.03251
Re	109,180	108,512	103,483
$y_{\max}^+$	156	176	148

**Table 3: Results of Sensitivity Study Comparing Standard and RNG k- $\epsilon$  Models with the RSM (4,908 cells).**

Parameter	Standard k- $\epsilon$	RNG k- $\epsilon$	RSM
Discretisation scheme	2nd Order	2nd Order	2nd Order
$C_d$	0.786	0.791	0.724
Difference from ESDU	11.8%	12.5%	3.0%
$U_{\max}$ , m.s <sup>-1</sup>	115.4	120.1	127.9
$W_{\text{actual}}$ , kg.s <sup>-1</sup>	0.03357	0.03380	0.03094
Re	106,857	107,589	98,485
$y_{\max}^+$	355	369	276

Following from this result, sensitivity studies comparing the RSM with the k- $\epsilon$  turbulence model, and the RSM with the RNG k- $\epsilon$  model are given in Tables 2 and 3. It can be seen that the RSM gives significantly better agreement with the ESDU values for  $C_d$  than either the standard or RNG k- $\epsilon$  turbulence models. The results in the tables show that with the RSM

the mass flow is smaller than with the k-ε models, despite a higher peak velocity in the orifice ( $U_{\max}$ ) implying a narrower vena contracta.

### 3 COMPRESSIBLE FLOW THROUGH A SHARP-EDGED SLIT

Information about the compressible flow through a sharp-edged slit was obtained from Shapiro (4). Shapiro presents theoretical values for  $C_d$  in terms of a contraction ratio for the two-dimensional flow through a slit. The contraction ratio is  $b/d$  where  $d$  is the width of the slit and  $b$  is the width of the of the emergent jet an infinite distance downstream. The contraction ratio was found to depend upon the exit jet Mach number,  $M$ ,

$$\frac{b}{d} = \frac{\pi}{\pi + 2\sqrt{1 - M^2}}. \quad (1)$$

For verification purposes, FLUENT solutions can provide exit jet Mach numbers, compressible flow  $C_d$ s (from simulation boundary conditions and the bulk mass flow rate) and estimates of contraction ratio from streamlines. Estimating  $b/d$  from solution streamlines is of particular importance as it provides a check that FLUENT is correctly simulating flow patterns in the vicinity of the slit.

The flow was simulated in two-dimensions using a symmetry plane along the slit centre. The model was meshed with between 270 and 22,819 triangular cells and with both first and second order discretisation schemes. With  $\Delta P=20\text{kPa}$  mesh refinement was carried out using a combination of  $y^+$  adaption and doubling (Figure 6). The effects on  $C_d$  are given in Figure 7. Above around 2000 cells the refinement has very little effect on  $C_d$ .

For the validation, the most accurate solution might be expected to be the one using 21,953 cells and a second-order discretisation scheme. This gave  $C_d=0.7760$  for  $M=0.53$ . At this Mach number, the theoretical  $C_d=0.649$  (equation 1) is for a slit placed in an infinite duct, so a correction must be applied to the simulated value to account for the 8cm width of the duct (a wider diameter duct was not used in the simulation in an attempt to keep down the number of cells required). The correction was derived using a generalised orifice model (5), which allowed the  $C_d$  for flow in both an infinite and 8cm wide duct to be calculated. The difference between these two results (0.151) was then subtracted from the computed value to give  $C_d=0.625$  for  $M=0.53$ . This lies 3.7% from the Shapiro value of  $C_d=0.649$  for  $M=0.53$ .

The generalised orifice model (5) was not used to calculate a  $C_d$  for comparison with the simulation directly because its absolute accuracy was not known. However it is hoped that any relative  $C_d$  values derived from it were sufficiently accurate for the present purpose.

It is slightly unsatisfactory that using Shapiro (4) as the data source for the validation has required the use of a correction to account for the infinite duct width used in the theory. However the theory included a relationship for the jet contraction ratio leaving the orifice, which allowed the simulated flow pattern to be partially validated. In the simulation a massless particle was released from the tip of the orifice, which under the steady conditions

used, traced a streamline for the flow (not shown). The resulting flow pattern gave satisfactory agreement with the theoretical result.

#### 4 CONCLUSIONS

For incompressible flow through orifices with an aspect ratio  $t/d=0.5$  CFD simulation can have difficulties correctly predicting the flow pattern and hence  $C_d$ s. While standard  $k-\epsilon$  and RNG turbulence models predicted the separation at the inlet lip of the orifice, they incorrectly predicted that flow would re-attach before leaving the orifice, leading to values of  $C_d$  11% or more too high. For the  $t/d=0.5$  aspect ratio orifice studies, the RSM calculated more accurate values for  $C_d$  by correctly predicting that flow would not re-attach before exiting the orifice. Accuracies of better than 4% were readily attained.

In the case of compressible flow through a sharp-edged slit the  $k-\epsilon$  turbulence model predicted the value of  $C_d$  to about 4% of the ESDU value.

#### 5 REFERENCES

1. Hay, N and Lampard, D (1996), Discharge coefficient of turbine cooling holes: a review, Transactions of the ASME, 96-GT-492.
2. User's guide for FLUENT/UNS & RAMPANT release 4.0. April 1996, Fluent Incorporated, Centerra Resource Park, 10 Cavendish Court, Lebanon, NH 03766, USA.
3. ESDU (Engineering Sciences Data Unit) Item Number 81039, Vol. 3a, Flow of liquids. Pressure losses across orifice plates, perforated plates and thick orifice plates in ducts, Approved for issue 1981 with amendments A and B, March 1985. Engineering Sciences Data Unit, 251-259 Regent Street, London, W1R 7AD, UK.
4. Shapiro (1953), The dynamics & thermodynamics of compressible fluid flow, Volume 1, ISBN 0-471-06691-5, Congress Card 53-8869.
5. Dodge (1964), Fluid throttling devices - flow resistance in piping and components, Product Engineering Reprint 109, McGraw-Hill, N.Y., 30 March 1964, pp14-20.

© With Author 1998



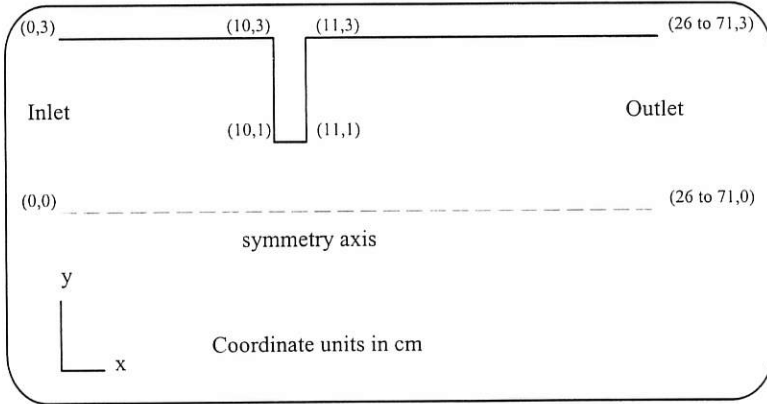


Figure 1: Two-Dimensional Axisymmetric Configuration.

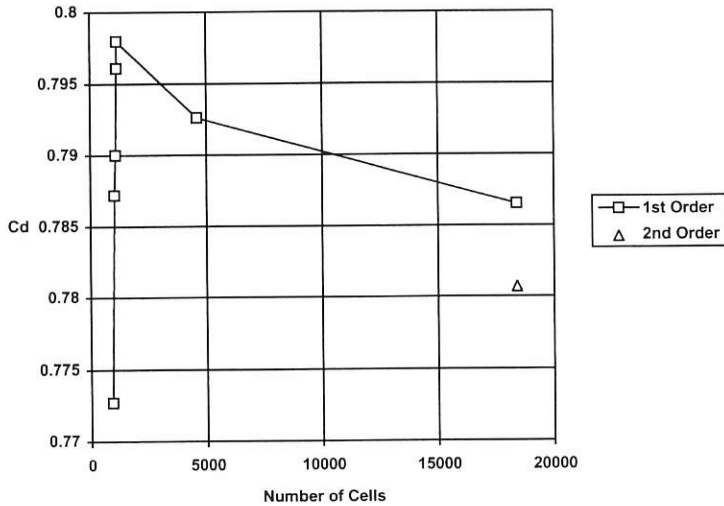
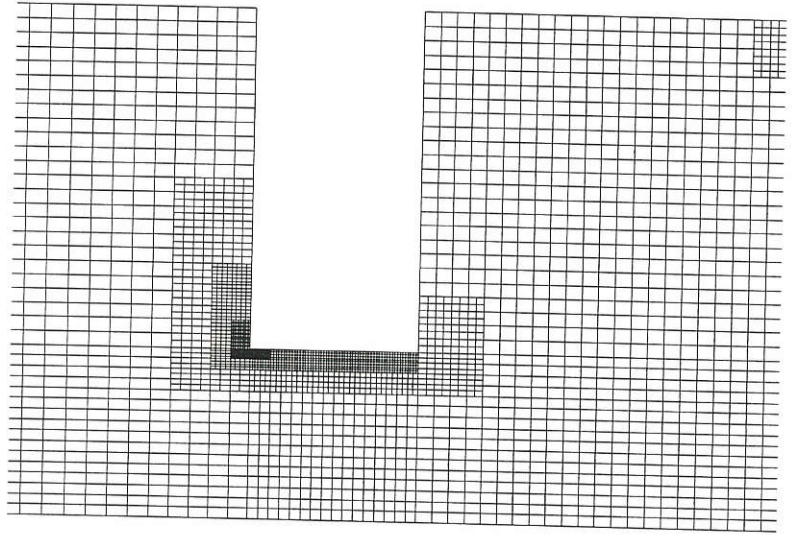


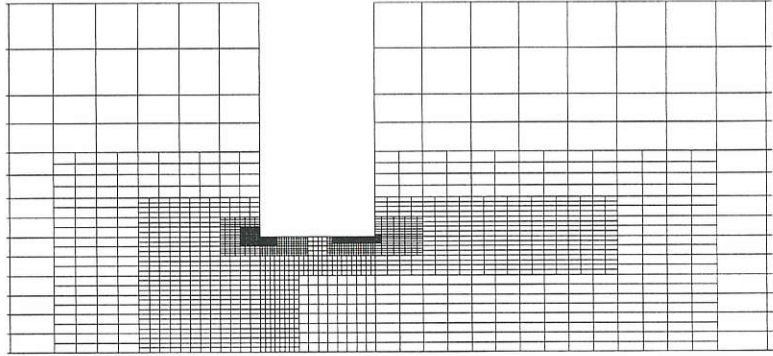
Figure 2: Axisymmetric Incompressible Flow. Effect of Mesh Refinement on  $C_d$ .



Grid

Fluent/UNS 4.2 (axi, ke)  
Thu Jun 11 1998  
Fluent Inc.

**Figure 3: Axisymmetric Incompressible Flow. Mesh Around Orifice Following Refinement to 18,400 Cells.**



Grid

Fluent/UNS 4.2 (axi, rsm)  
Thu Jun 11 1998  
Fluent Inc.

**Figure 4: Mesh of 3,787 Cells with Refinement Carried out in Advance of Simulation.**

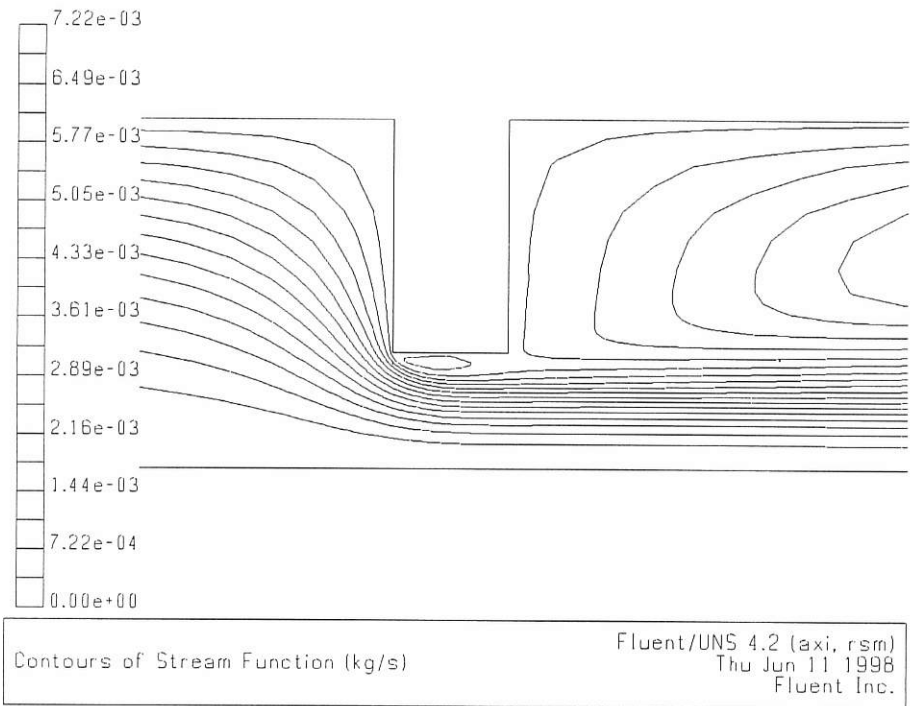
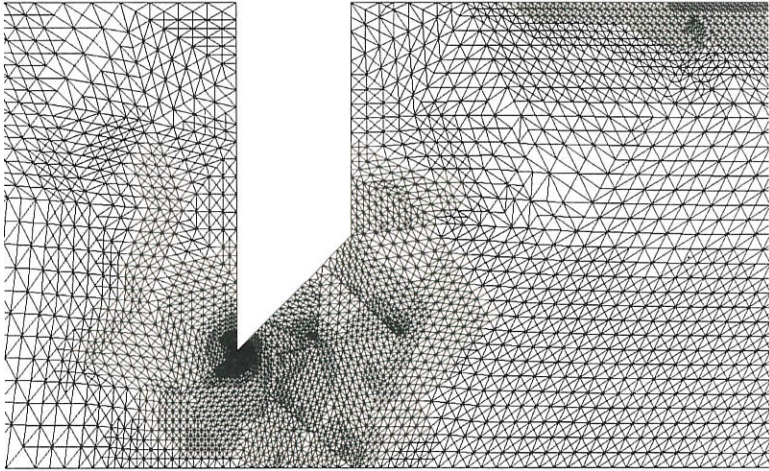


**Figure 5: Streamlines of Incompressible Orifice Flow Using RSM and 3,787 Cells.**



Grid

Fluent/UNS 4.2 (2d, rsm)  
Thu Jun 11 1998  
Fluent Inc.

**Figure 6: Two-Dimensional Compressible Flow, Triangular Mesh Around Slit After Adaption to 22,819 Cells.**

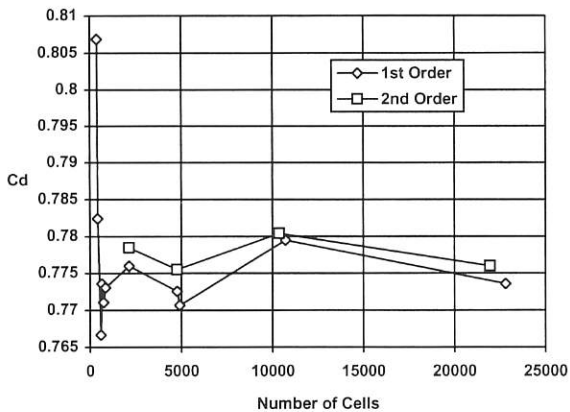


**Figure 7: Two-Dimensional Compressible Flow, Triangular Mesh. Effect of Refinement on  $C_d$ .**